

A negative cosmological constant in the dark sector?

Rodrigo Calderón,^{1,*} Radouane Gannouji,^{2,†} Benjamin L’Huillier,^{3,‡} and David Polarski^{1,§}

¹*Laboratoire Charles Coulomb, Université de Montpellier & CNRS*

²*Instituto de Física, Pontificia Universidad Católica de Valparaíso, Av. Brasil 2950, Valparaíso, Chile*

³*Department of Astronomy, Yonsei University, 50 Yonsei-ro, Seodaemun-gu, Seoul 03722, Korea*

(Dated: December 22, 2024)

We consider the possibility that the dark sector of our universe contains a negative cosmological constant dubbed λ . For such models to be viable, the dark sector should contain an additional component responsible for the late-time accelerated expansion rate (X). We explore the departure of the expansion history of these models from the concordance Λ CDM model. For a large class of our models the accelerated expansion is transient with a nontrivial dependence on the model parameters. All models with $w_X > -1$ will eventually contract and we derive an analytical expression for the scale factor $a(t)$ in the neighbourhood of its maximal value. We find also the scale factor for models ending in a Big Rip in the regime where dustlike matter density is negligible compared to λ . We address further the viability of such models, in particular when a high H_0 is taken into account. While we find no decisive evidence for a nonzero λ , the best models are obtained with a phantom behaviour on redshifts $z \gtrsim 1$ with a higher evidence for nonzero λ . An observed value for h substantially higher than 0.70 would be a decisive test of their viability.

I. INTRODUCTION

While the physical mechanism behind the late-time accelerated expansion rate of the Universe still remains an open question [1–4], its phenomenology is known with ever increasing accuracy [5, 6]. It is interesting that perhaps the simplest model, the Λ CDM model, where gravity is described by general relativity whereas dark energy (DE) is simply a positive constant Λ , can account for the data to some accuracy. Hence the concordance model in which the present accelerated expansion rate is driven by a cosmological constant Λ has become the reference cosmological model. Aside from the theoretical problems, the smallness of Λ compared to expected Planckian values, it is not clearly established whether this model can successfully cope with all observations especially on small cosmic scales (see e.g. [7]). Hence one is still investigating other DE models, both inside and outside general relativity, which are able to roughly reproduce the Λ CDM phenomenology and are therefore viable with the hope that some specific signature will single them out. Recently the so-called tensions with the concordance model, and more generally possible discrepancies [8] between early and late time measurements of cosmic quantities, have attracted a lot of interest with a special emphasis on the H_0 tension [9–13]. This latter tension – a substantial difference at the $\sim 4\sigma$ level between the value of the present Hubble constant H_0 derived from the Cosmic Microwave Background (CMB) Planck data [14] on one hand and from local data on the other hand, when the concordance model is assumed – could imply that the DE sector is more complicated

than in the concordance model. This is one more incentive to consider models which are more sophisticated than Λ CDM. It is well known on the other hand that the presence of a positive cosmological constant Λ in superstring models is problematic. These theories prefer a negative cosmological constant, dubbed here λ , reflecting the embedding of the Anti de Sitter rather than the de Sitter symmetry group. It is therefore interesting to investigate the possibility that our homogeneous expanding Universe contains a λ term and it may come as a surprise that this is indeed viable. In some sense this is so as long as the presence of the λ term does not change radically the main properties of the expansion history of our Universe compared to the concordance model. This requires first of all that the (smooth) dark sector (which we call here for simplicity the DE sector) contains an additional component, dubbed here X component, responsible for the late-time accelerated expansion rate (see e.g. [15, 16]). Note that a transient effective λ switching around recombination to a positive Λ was considered in [17] while [18] considers the intriguing possibility of such a spontaneous switch at $z \sim 2$. Let us mention that a negative, not necessarily constant, energy component can also appear as a result of the equations of motion like the negative dark radiation component found in [19]. Among other interesting examples of components that can have negative energy is the “missing matter” of [20], the dynamical $\Lambda(t)$ term in [21], or the reconstructed total dark energy component (see e.g. [22]).

We address in this work the observational viability in the presence of a negative λ term for several behaviours of the dark sector, investigating more specifically the constraint coming from a high H_0 . Independently of observations, we study also the future evolution of such Universes with constant w_X , in which case a λ term can crucially change the dynamics of our Universe. We address as well the non-trivial appearance of transient accelerated stages in the past.

* rodrigo.calderon-bruni@umontpellier.fr

† radouane.gannouji@pucv.cl

‡ blhuillier@yonsei.ac.kr

§ david.polarski@umontpellier.fr

II. COSMIC EXPANSION WITH A NEGATIVE COSMOLOGICAL CONSTANT

We recall first the basic equations and concepts. We intend to study here a universe containing a *negative* cosmological constant λ . Obviously, such a model cannot accelerate the late-time expansion rate of the Universe in the absence of some additional component in the dark sector. To comply with observations we add an X component with $w_X < -\frac{1}{3}$ on very low redshifts. For a spatially flat Friedmann-Lemaître-Robertson-Walker (FLRW) universe, the evolution of the Hubble parameter as a function of the redshift $z = \frac{a_0}{a} - 1$ at $z \ll z_{eq}$ reads

$$H^2(z) = H_0^2 [\Omega_{m,0} (1+z)^3 + \Omega_{\lambda,0} + \Omega_{X,0} f_X(z)] , \quad (1)$$

where $H(t) \equiv \dot{a}(t)/a(t)$ is the Hubble parameter, a is the scale factor and a dot stands for the derivative with respect to cosmic time t , $\Omega_i \equiv \frac{\rho_i}{\rho_{cr}}$ with $3H^2 \equiv 8\pi G\rho_{cr}$, finally $f_X(z) = \frac{\rho_X(z)}{\rho_{X,0}}$ is given by

$$f_X(z) = \exp \left[3 \int_0^z dz' \frac{1 + w_X(z')}{1 + z'} \right] , \quad (2)$$

with $w_X \equiv p_X/\rho_X$. When we consider later constraints involving much larger redshifts, we will add radiation and neutrinos. It is crucial that in (1) we have

$$\Omega_{\lambda,0} < 0 , \quad (3)$$

as we assume the presence of a negative cosmological constant $\lambda < 0$. For such a model it is natural to make the following identification

$$\Omega_{DE,0} \equiv \Omega_{\lambda,0} + \Omega_{X,0} \simeq 1 - \Omega_{m,0} . \quad (4)$$

The combined dark energy (DE) sector must of course be able to produce the late-time accelerated expansion of the universe.

While a negative cosmological constant can hide in the dark sector during the past evolution of our Universe, it can significantly modify its future evolution. Before considering the asymptotic future it is also very interesting to study the appearance of accelerated stages in such models.

A. Transient accelerated stages

The inclusion of a negative cosmological constant has various interesting features. In this subsection, we study some of its generic properties independent of any observational constraints.

Let us first remember that for a model of universe composed by matter and dark energy with a constant equation of state parameter w , the universe accelerates today for $w < -1/(3\Omega_{DE,0})$ which, for example, gives $w < -0.48$ if $\Omega_{DE,0} = 0.7$. In the presence of two fluids,

the problem becomes more complicated. In our case, we consider a negative cosmological constant and a constant equation of state, w_X , for the X -component. The condition of an acceleration of the universe today reduces to

$$w_X < \frac{\Omega_{\lambda,0} - 1/3}{1 - \Omega_{m,0} - \Omega_{\lambda,0}} . \quad (5)$$

We have an additional degree of freedom, $\Omega_{\lambda,0}$. In fact even if $\Omega_{\lambda,0} + \Omega_{X,0}$ is fixed (to 0.7 for example), $\Omega_{\lambda,0}$ is free to take any value. Considering $\Omega_{\lambda,0} < 0$, we find that the universe accelerates today for some value of w_X in the range $-1 < w_X < -0.48$ depending on the value of $\Omega_{\lambda,0}$. For a large negative value of $\Omega_{\lambda,0}$, we need a more negative w_X , with $w_X \rightarrow -1$, in order to produce an acceleration today. Considering now the more complicated situation of an acceleration of the universe not only today but which could occur at any time, we find some peculiar results when $\Omega_{\lambda,0} < 0$. First, it is trivial to see that during the matter era, the two fluids are negligible (assuming $w_X < 0$) and therefore the universe decelerates. In the future, if the X component is not phantom, the negative cosmological constant eventually dominates and we have recollapse and therefore a non-accelerating universe. Only if the X component is phantom, we will have acceleration in the asymptotic future. Considering the situation where the X component is not phantom, we have deceleration in the past and in the future. Therefore, we conclude that for non-phantom dark energy with a negative cosmological constant, if the universe accelerates, it will always be transient. To have an acceleration, we need the situation where dark energy starts to dominate over matter, which always happens at some cosmic time, but it should be sufficiently large at that time in comparison to the negative cosmological constant, otherwise the expansion of the universe would always be decelerated. We see in Fig. 1 the maximum of the acceleration reached by the universe from matter era until today is shown while we assume for illustration $\Omega_{m,0} = 0.3$. For $\Omega_{\lambda,0} = -2$, we observe that if $-1 < w_X < -0.84$, there is an epoch during which we have acceleration while for $-0.84 < w_X < -0.5$, the universe always decelerates until today. This follows our standard intuition: we need w_X sufficiently negative to produce an acceleration. On the other hand, for $\Omega_{\lambda,0} = -7$, we observe a more complicated structure. For $-1 < w_X < -0.93$ and $-0.82 < w_X < -0.54$ the universe reached in the past or today a phase of acceleration, while for $-0.93 < w_X < -0.82$ and $-0.54 < w_X$, the universe never accelerated in the past. The maximum value for \ddot{a}/a , assuming only w_X constant, is given by

$$\left. \frac{\ddot{a}}{H_0^2 a} \right|_{\max} = \Omega_{\lambda,0} - \frac{w_X \Omega_{m,0}}{2(1 + w_X)} \left[\frac{\Omega_{X,0}(1 + 3w_X)(1 + w_X)}{-\Omega_{m,0}} \right]^{-\frac{1}{w_X}} , \quad (6)$$

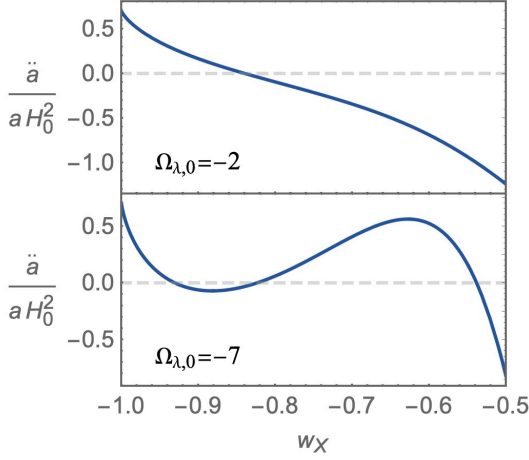


FIG. 1. Evolution of the maximum value of \ddot{a}/a reached from matter era until today, as a function of w_X for two different values of $\Omega_{\lambda,0}$ and $\Omega_{m,0} = 0.3$.

which shows the nontrivial dependence of the acceleration parameter on w_X and $\Omega_{\lambda,0}$. In Fig. 2, we extended this analysis to a large range of $\Omega_{\lambda,0}$ and w_X and assuming $\Omega_{m,0} = 0.3$. In white, the universe accelerates today while in gray the universe decelerates today. The latter is divided in areas (light gray) where the universe never accelerated until today and situations (darker gray) where the universe had an acceleration in the past but does not accelerate today.

Having in mind the observational constraints which will be addressed more thoroughly later, we have also represented in the same figure the set of parameters satisfying Eq. (26) in red for $h = 0.74$ and in purple for $h = 0.72$. Notice that if $\Omega_{\lambda,0} = 0$, we need $w_X = -1.2$ to obtain $h = 0.74$ as it was already noticed in [23]. For negative values of the cosmological constant the required phantomness is milder as we will see in Section III.

B. Future asymptotic solutions

Let us consider now the limit in the future where dust-like matter density becomes negligible compared to the dark sector density. As we have our Universe in mind, we consider the regime in the future for which $\Omega_{m,0} \left(\frac{a_0}{a}\right)^3 \ll |\Omega_{\lambda,0}| < \Omega_{X,0}$. Then, we have to solve the effective Friedmann equation

$$H^2 = -|\alpha| + \frac{\beta}{a^p}, \quad (7)$$

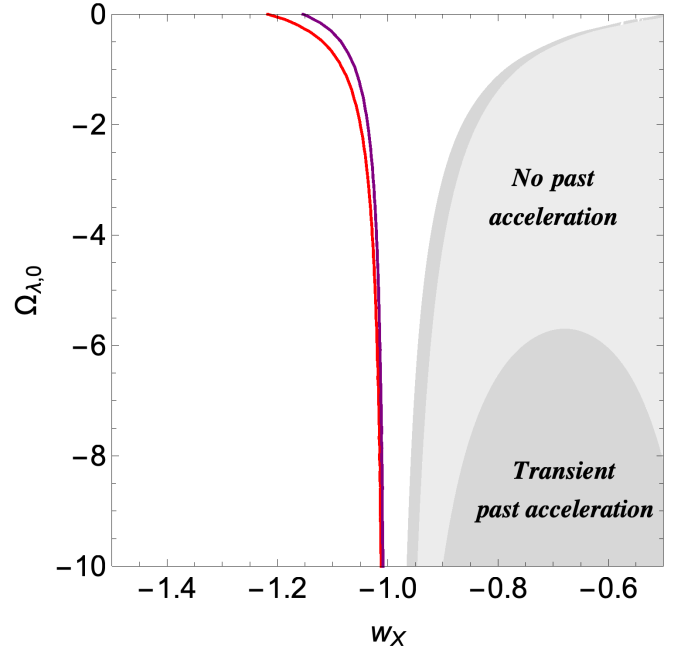


FIG. 2. Evolution of the universe in the space $(w_X, \Omega_{\lambda,0})$. In white, the universe accelerates today, in light gray, the universe never accelerated until today while in darker gray, we have a transient situation where the universe accelerated in the past but does not accelerate today. These results do not rely on any observational constraints, only $\Omega_{m,0} = 0.3$ and w_X constant are assumed. For comparison, we have added in red and purple lines the $(\Omega_{\lambda,0}, w_X)$ values which satisfy Eq. (26) for $h = 0.74$ and $h = 0.72$ respectively.

where we have set for brevity

$$\begin{aligned} \alpha &\equiv \Omega_{\lambda,0} H_0^2 < 0 \\ \beta &\equiv \Omega_{X,0} H_0^2 a_0^p \\ p &\equiv 3(1 + w_X). \end{aligned} \quad (8)$$

The exact solution of Eq. (7) is

$$a = \left(\frac{\beta}{|\alpha|} \right)^{\frac{1}{p}} \sin^{\frac{2}{p}} \left(\frac{p}{2} \sqrt{|\alpha|} t + C \right), \quad (9)$$

or more explicitly in function of the cosmological parameters

$$\frac{a}{a_0} = \left(\frac{\Omega_{X,0}}{|\Omega_{\lambda,0}|} \right)^{\frac{1}{p}} \sin^{\frac{2}{p}} \left(\frac{p}{2} \sqrt{|\Omega_{\lambda,0}|} H_0 t + C \right), \quad (10)$$

where C is an integration constant. We obtain further

$$\frac{H}{H_0} = \sqrt{|\Omega_{\lambda,0}|} \cot \left(\frac{p}{2} \sqrt{|\Omega_{\lambda,0}|} H_0 t + C \right) \quad (11)$$

$$\frac{\dot{H}}{H_0^2} = \frac{p}{2} |\Omega_{\lambda,0}| \left[-1 - \cot^2 \left(\frac{p}{2} \sqrt{|\Omega_{\lambda,0}|} H_0 t + C \right) \right] \quad (12)$$

If $p = 0$ ($w_X = -1$), the two terms on the r.h.s. of Eq. (7) combine to give an effective positive cosmological constant. The resulting future evolution is that of

Λ CDM. Note that it is possible in this case to give the exact analytic expression even when dustlike matter is taken into account.

We consider next $p > 0$, in other words the X -component is not of the phantom type. As its density is decreasing with expansion, the universe will eventually recollapse. Note that the density of dustlike matter decreases even more rapidly ($\propto a^{-3}$) so Eq. (7) applies if $|\Omega_{\lambda,0}| \ll \Omega_{\text{DE},0} \approx 0.7$ and $w_X \approx -1$. Indeed, we can read off from Eq. (10) the condition for the existence of a time interval before the contraction during which dustlike matter can be neglected, viz.

$$\left(\frac{|\Omega_{\lambda,0}|}{|\Omega_{\lambda,0}| + \Omega_{\text{DE},0}} \right)^{\frac{3}{p}} \ll \frac{|\Omega_{\lambda,0}|}{\Omega_{\text{m},0}} \quad (13)$$

As expected, we verify further with Eqs. (11), (12), that the expansion is decelerating, $\ddot{a} < 0$, (at least) in the neighbourhood of a_M , the maximal value of the scale factor. As expected this is only so for $0 < p < 2$ ($-1 < w_X < -\frac{1}{3}$) otherwise there is no acceleration at all. So even if the universe is accelerating today, it passes again through $\ddot{a} = 0$, from an accelerating to a decelerating expansion rate. When (13) is satisfied, this takes place at

$$\frac{a_M}{a} \simeq \left(1 + \frac{p}{2} \right)^{\frac{1}{p}}, \quad (14)$$

which is close to a_M and lies in the regime described by (7).

We now turn to $p < 0$, the phantom case. It is clear that the universe will eventually reach the Big Rip singularity in a finite time t_∞ . In some range before t_∞ , the dust-like component will be negligible compared to the negative cosmological constant. In that case, $a(t)$ is given to high accuracy by the solution (9) or (10). To ensure the presence of a Big Rip at t_∞ , we write the integration constant C in a way to have a Big Rip at $t = t_\infty$ and the solution for $a(t)$ then reads

$$a(t) = \left(\frac{|\Omega_{\lambda,0}|}{\Omega_{X,0}} \right)^{\frac{1}{|p|}} a_0 \sin^{-\frac{2}{|p|}} \left(\frac{|p|}{2} \sqrt{|\Omega_{\lambda,0}|} H_0 (t_\infty - t) \right). \quad (15)$$

We verify easily that in the limit $t \rightarrow t_\infty$, this solution tends asymptotically to

$$a(t) \sim \frac{A}{(t_\infty - t)^{\frac{2}{|p|}}}, \quad (16)$$

with A given by

$$A = \left(\frac{|p|}{2} \sqrt{\Omega_{X,0}} H_0 \right)^{-\frac{2}{|p|}} a_0. \quad (17)$$

This is the well-known singular behaviour in the vicinity of t_∞ , depending solely on the phantom component, here the X component. The solution (15) gives a nearly exact fit in the regime $\Omega_{\text{m},0} \ll |\Omega_{\lambda,0}|$ and improves on (17) when t is sufficiently far from t_∞ .

III. COSMIC RELEVANCE OF λ AND THE H_0 TENSION

We now turn to the cosmic relevance of models admitting a negative cosmological constant λ . As for any cosmological model differing from Λ CDM, an important question to address is how viable the model is if the measured value of h is substantially higher than 0.67. It is well known that there is a tension between the value of H_0 obtained by Planck and the value obtained with many local (low redshifts) measurements. This is a very interesting problem which has been widely investigated recently in various ways (see e.g. [24–41] for a non exhaustive list). This tension can be traced back to the measurement of the standard ruler r_s , the comoving sound horizon at recombination time (very close to the drag epoch) relevant for the corresponding angle θ_s sustained on the CMB

$$r_s(z_1) = \int_0^{t_1} c_s \frac{dt}{a(t)} = \frac{1}{a_0} \int_{z_1}^\infty c_s \frac{dz}{H(z)}, \quad (18)$$

where adiabatic primordial fluctuations are assumed. The angle θ_s is given by

$$\theta_s = \frac{a_1 r_s(z_1)}{d_A(z_1)}, \quad (19)$$

where $d_A(z)$ is the angular-diameter distance out to a redshift z . We finally obtain

$$\theta_s = \frac{r_s(z_1)}{r(z_1)}, \quad (20)$$

with

$$r(z_1) = \frac{c}{a_0} \int_0^{z_1} \frac{dz}{H(z)}. \quad (21)$$

We have written explicitly the light velocity c and a_0 in (18), (21) ($c = 1$ and $a_0 = 1$ in this work but will sometimes be written explicitly). We choose the Planck 2018 TT,TE,EE+LowE+Lensing constraints (no BAO), with one massive neutrino species [42]. We take the redshift $z_1 = z_{\text{rec}} = 1089.92$, $\theta_s^{\text{Planck}} = 1.04110 \times 10^{-2}$, $r_s^{\text{Planck}}(z_{\text{rec}}) = 144.43 \text{ Mpc}$, see Table I.

The relative energy density $\Omega_{i,0} \equiv \frac{\rho_{i,0}}{\rho_{\text{cr},0}}$, defined as

$$\Omega_{i,0} = \frac{8\pi G \rho_{i,0}}{3H_0^2}, \quad (22)$$

suffers from the uncertainty of the value of H_0 even if ρ_i is otherwise known. However, it is often possible to find observationally the numerical value of the combined quantities

$$\omega_i \equiv \Omega_{i,0} h^2, \quad (23)$$

with $h \equiv \frac{H_0}{100 \text{ km s}^{-1} \text{ Mpc}^{-1}}$. For our models, we have obviously at low redshifts

$$H(z) = [\omega_m (1+z)^3 + \omega_\lambda + \omega_X f_X(z)]^{\frac{1}{2}} \times 100 \text{ km s}^{-1} \text{ Mpc}^{-1}. \quad (24)$$

In the standard Λ CDM model, the value of $r_s(z_1)$ is controlled by the quantities ω_i contained in the model with the notable exception of ω_Λ . Measuring these quantities yields in turn $r_s^{\text{Planck}}(z_1)$. As the angle θ_s^{Planck} is accurately measured by the Planck collaboration, the numerical value of $r(z_1)$ becomes fixed in turn (for given θ_s measured by Planck) to its value $r^{\text{Planck}}(z_1)$,

$$r^{\text{Planck}}(z_1) = 13\,872.8 \text{ Mpc} . \quad (25)$$

Hence, once a cosmological model is adopted which does not change the early-time physics of Λ CDM, such a model is compelled to give the same $r(z_1)$. For Λ CDM this boils down to fix the value $\omega_\Lambda^{\text{Planck}}$ and therefore the value of H_0 . The Planck collaboration finds $H_0 = 67.36 \text{ km s}^{-1} \text{ Mpc}^{-1}$ a value substantially lower than the value measured locally. We refer the interested reader to the excellent account given in [43].

In this work we are interested in models which depart from Λ CDM regarding the universe expansion for $z < z_1$, however in a way that they satisfy

$$r(z_1) = r^{\text{Planck}}(z_1) \quad (26)$$

for a *larger* H_0 value. At this stage we emphasize two points: first, as we have said earlier, when we compare our models with data we fix r_s , and hence we must also fix ω_m and ω_r , to their fiducial Planck values. A more elaborate analysis could be performed by allowing all ω_i 's to vary. We feel the constraint on our models is essentially expressed with our simpler analysis at this stage. Second, in our theoretical investigations performed below in Section III (see Fig. 3 and Fig. 4), the constraint (26) is used, assuming that both r_s and θ_s are fixed to their Planck values (see Table I). In the comparison with observations performed in Section IV, r_s , ω_m and ω_r are fixed and we consider the measured θ_s with its associated error hence $r(z_1)$ can vary around the value (25). We can then compare $\theta_s^{\text{theory}} = r_s/r(z_1)$ with the Planck measured value $\simeq 1.04 \times 10^{-2}$, constraining ω_X , ω_λ and ultimately h .

It is obvious from (24), (20) that a larger H_0 requires

$$\omega_{\text{DE}} = \omega_\lambda + \omega_X > \omega_\Lambda^{\text{Planck}} , \quad (27)$$

and a phantom behaviour of the X component, hence also an effective phantom behaviour of the DE sector. This amounts to explore models with $w_X < -1$ at least during part of the late-time expansion. It is straightforward to obtain the exact equality

$$\omega_{\text{DE}} - \omega_\Lambda^{\text{Planck}} = h^2 - (h^{\text{Planck}})^2 , \quad (28)$$

It is further clear that our models satisfy (by construction)

$$\Omega_{\text{m},0} = \left(\frac{h^{\text{Planck}}}{h} \right)^2 \Omega_{\text{m},0}^{\text{Planck}} < \Omega_{\text{m},0}^{\text{Planck}} \quad (29)$$

$$\Omega_{\text{DE},0} \simeq 1 - \Omega_{\text{m},0} > \Omega_{\Lambda,0}^{\text{Planck}} . \quad (30)$$

Since we have to calculate distances up to $z = z_{\text{rec}}$, where radiation is subdominant but not negligible, we have to properly take into account the effect of photons and neutrinos. At high redshifts ($z \gtrsim 50$), Eq. (24) becomes [44]

$$\frac{H(z)}{100 \text{ km s}^{-1} \text{ Mpc}^{-1}} = \left[\omega_m (1+z)^3 + \omega_\lambda + \omega_X f_X(z) + \omega_\gamma (1+z)^4 \left(1 + 0.2271 \frac{N_{\text{eff}}}{3} \sum_i f_\nu \left(\frac{m_{\nu_i}}{T_\nu} \right) \right) \right]^{\frac{1}{2}} , \quad (31)$$

with $\omega_\gamma = 2.47 \times 10^{-5}$ while f_ν is well fitted with $f_\nu(y) \simeq (1 + (Ay)^p)^{1/p}$ with $A = \frac{180\zeta(3)}{7\pi^4}$ and $p = 1.83$ [44]. The function f_ν interpolates between the relativistic behaviour, $m_\nu \ll T_\nu$ ($T_\nu \sim a^{-1}$), and the non-relativistic regime, $m_\nu \gg T_\nu$. Even for m_ν as light as 0.06eV, the transition occurs rather early around $z \simeq 110$. Given these considerations, we fix the early Universe cosmology as in table I.

$100 \omega_b$	$100 \omega_c$	N_{eff}	m_ν (eV)	r_s (Mpc)	r_d (Mpc)	$100 \theta_s$
2.237	12.00	3.046	(0,0,0.06)	144.43	147.09	1.04110

TABLE I. Parameter values as given by the Planck 2018 TT,TE,EE+LowE+lensing results (Table 2). r_s is the comoving sound horizon at recombination ($z_1 = 1089.92$), and r_d at the drag epoch $z_d = 1059.94$

A. Models

When assessing the viability of our models with respect to the low-redshift data and the constraint on their free parameters coming from a high H_0 , we will consider various types of equation of state (EoS) parameters w_X and various values of ω_λ .

Scenario w : We consider first models with constant equation of state $w_X = \text{constant}$. In this case we obviously have

$$f_X(z) = (1+z)^{3(1+w_X)} . \quad (32)$$

As we have seen earlier, to ease the H_0 tension necessarily requires a phantom behaviour and for a constant w_X the only possible choice is to take $w_X < -1$. We take an EoS of the form

$$w_X = -1 + \Delta_1 = w_0 , \quad \Delta_1 < 0 , \quad (33)$$

and we obtain immediately

$$f_X(z) = (1+z)^{3\Delta_1} . \quad (34)$$

While a constant w_X gives us some insight, it is clearly advisable to explore also models with varying equations of state.

CPL scenarios: here we adopt the CPL parametrization of w_X corresponding to a smoothly (differentiable) varying EoS with

$$w_X = w_0 + w_a(1 - a) \equiv -1 + \Delta + w_a(1 - a) \quad (35)$$

which gives [45],[46]

$$f_X(z) = (1 + z)^{3(\Delta + w_a)} \exp^{-3w_a \frac{z}{1+z}}. \quad (36)$$

We consider also two constrained versions: CPL w_a , with $w_0 = -1$ while w_a is free; and CPL w_0 , where w_0 is free and $w_a = -1 - w_0$ so that $w_X \rightarrow -1 \equiv w_\infty$.

Scenario I: In this scenario, we take a piece-wise constant w_X where dark energy is of a phantom type below some transition redshift z_c and a cosmological constant Λ above, with

$$w_X(z) = \begin{cases} -1 + \Delta_1 = w_0, & \text{for } z \leq z_c \\ -1 = w_\infty, & \text{for } z > z_c \end{cases} \quad \Delta_1 < 0 \quad (37)$$

Here we take $\Delta_1 < 0$ in order to ensure a phantom behaviour and we fix $z_c = 1$. As z_c increases, it is easier to meet the data on small redshifts but it requires stronger phantomness on large redshifts in order to comply with the observed θ_s and a higher H_0 . We note that most of the SN Ia data are in the range $z_c \leq 1$. In this scenario, the evolution of the X-component is given by

$$f_X(z) = \begin{cases} (1 + z)^{3\Delta_1}, & \text{for } z \leq z_c \\ (1 + z_c)^{3\Delta_1}, & \text{for } z > z_c \end{cases} \quad (38)$$

Scenario II: This scenario has also a piece-wise constant w_X , but it is now opposite to the previous scenario, i.e.

$$w_X(z) = \begin{cases} -1 = w_0, & \text{for } z \leq z_c \\ -1 + \Delta_2 = w_\infty, & \text{for } z > z_c \end{cases} \quad \Delta_2 < 0 \quad (39)$$

We have now

$$f_X(z) = \begin{cases} 1, & \text{for } z \leq z_c \\ \left(\frac{1+z}{1+z_c}\right)^{3\Delta_2}, & \text{for } z > z_c \end{cases} \quad (40)$$

In this case too, we take $z_c = 1$.

Scenario III:

$$w_X(z) = \begin{cases} -1 + \Delta_1 = w_0, & \text{for } z \leq z_{c1} \\ -1, & \text{for } z_{c1} < z \leq z_{c2} \\ -1 + \Delta_2 = w_\infty, & \text{for } z > z_{c2} \end{cases} \quad \begin{matrix} \Delta_1 < 0 \\ \\ \Delta_2 < 0 \end{matrix} \quad (41)$$

We have in this case

$$f_X(z) = \begin{cases} (1 + z)^{3\Delta_1}, & \text{for } z \leq z_{c1} \\ (1 + z_{c1})^{3\Delta_1}, & \text{for } z_{c1} < z \leq z_{c2} \\ \frac{(1 + z_{c1})^{3\Delta_1}}{(1 + z_{c2})^{3\Delta_2}} (1 + z)^{3\Delta_2}, & \text{for } z > z_{c2} \end{cases} \quad (42)$$

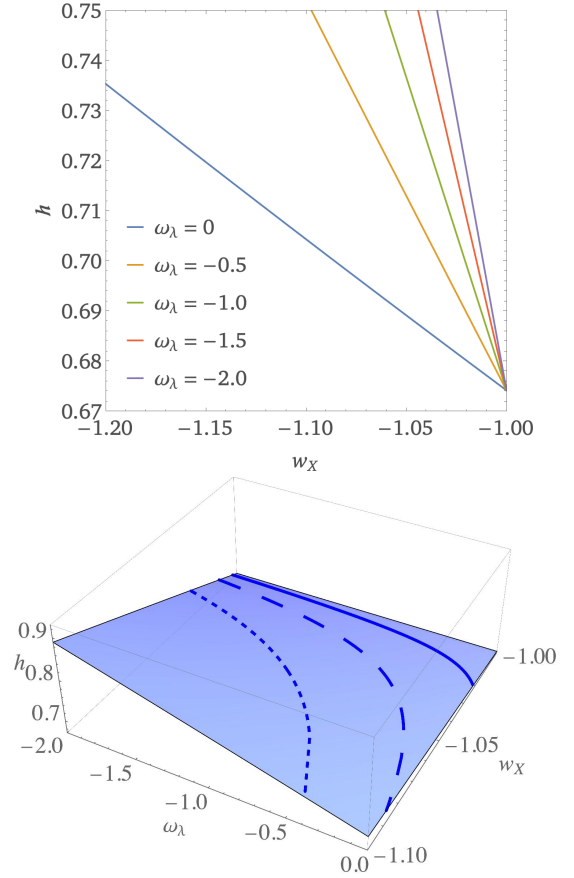


FIG. 3. Parameters (h, ω_λ, w_X) which satisfy the relation (26) for models with constant w_X . a) In the upper panel, ω_λ is fixed and we see that an increasing $|\omega_\lambda|$ (from left to right) gives the same h with less phantomness. We note the quasi-linear relation, which follows from (43) for constant ω_λ . b) In the lower panel all parameters are free. For the latter, we show the lines corresponding to a constant h when (26) is satisfied: continuous line ($h = 0.68$), long dashed line ($h = 0.7$) and dashed line ($h = 0.74$). They satisfy to good accuracy (43).

For this scenario we take $z_{c1} = 0.1$ and $z_{c2} = 1$. A significant change in w_X on very small redshifts is viable and we exploit also this possibility here.

Once a specific model is adopted we can find the dependence of h on the model parameters for a model satisfying (26). This gives insight into the phenomenology of these models irrespective of the observational constraints.

For constant w_X , we can study its behaviour in terms of the following three free parameters: ω_λ , w_X and h . Indeed the parameter ω_X is fixed once ω_λ and h are given. From the constraint (26) however, only two free parameters are left. In Figure 3, we show the value of h in terms of w_X , when ω_λ is fixed and as a function of w_X and ω_λ in a 3-dim plot. In the first case, we confirm the linear relation obtained in [23] (for $\omega_\lambda = 0$), which we

have generalized here to

$$h = 0.673 + (w_X + 1)(0.93\omega_\lambda - 0.33). \quad (43)$$

At this point we emphasize another interesting aspect of our models which we discuss here for a constant w_X . As we will see later, observations favour models of the phantom type, $w_X < -1$. This implies that $\rho_{\text{DE}} = \rho_\lambda + \rho_X$ will necessarily become negative in the past at some redshift z_λ and it is straightforward to find

$$1 + z_\lambda = \left[1 + \frac{h^2 - \omega_m}{|\omega_\lambda|} \right]^{-\frac{1}{3(1+w_X)}}. \quad (44)$$

We have used $\omega_{\text{DE}} \approx h^2 - \omega_m$ which is valid to high accuracy. On the other hand, $H^2(z)$ is necessarily positive $\forall z > z_m$ with

$$1 + z_m = \left[\frac{|\omega_\lambda|}{\omega_m} \right]^{\frac{1}{3}}. \quad (45)$$

It is seen from (44) that $z_\lambda \rightarrow 0$ as $|\omega_\lambda|$ is increasing and w_X is more phantom. When this is the case there might be some parameter values for which $H^2(z)$ itself becomes negative for some redshifts in the range $z_\lambda < z < z_m$, such models are not viable and must be rejected. The condition $H^2(z) > 0$ is easily translated into

$$\omega_m [(1+z)^3 - f_X(z)] + h^2 f_X(z) > |\omega_\lambda| (1 - f_X(z)). \quad (46)$$

This inequality depends on the free parameters w_X , ω_λ , h . However, we should remember that in our theoretical analysis once w_X and ω_λ are given, because of the constraint (26) h is no longer free as we illustrate with Figures 3 and 4. We see that a priori, for given w_X , large $|\omega_\lambda|$ and low h^2 values can lead to a violation of (46). Once a two-dimensional surface $h(w_X, \omega_\lambda)$ is found satisfying (46) (see the lower panel of Figure 3), the projection in the (w_X, ω_λ) plane satisfies it automatically too.

IV. COMPARISON WITH DATA: MODEL SELECTION AND PARAMETER ESTIMATION

In this section, we are interested in the question of model selection: namely, comparing the different models to the reference Λ CDM model. Let M be the model, D the data, and Θ the parameters of the model. Bayes theorem can be written as

$$\Pr(\Theta|M, D) = \frac{\Pr(D|\Theta, M) \Pr(\Theta|M)}{\Pr(D|M)}, \quad (47)$$

where $\mathcal{P}(\Theta) = \Pr(\Theta|M, D)$ is the posterior distribution, $\mathcal{L}(\Theta) = \Pr(D|\Theta, M)$ is the likelihood, $\pi(\Theta) = \Pr(\Theta|M)$ is the prior, and $\mathcal{Z} = \Pr(D|M)$ is the evidence.

For parameter evaluation within a given model, the evidence can be seen as a normalization constant, and

Models	parameter	prior range
all	h	$[0.5, 1]$
λ all	ω_λ	$[-4, 0]$
$(\lambda)w/\text{I/III/CPL}w_0$	w_0	$[-1.2, -0.8]$
$(\lambda)\text{II/III}$	w_∞	$[-1.2, -0.8]$
$(\lambda)\text{CPL}w_a$	w_a	$[-0.2, 0.2]$

TABLE II. Flat prior range used in the nested sampling. For each model, (λ) denotes both cases with and without λ

thus ignored. However, in order to perform model selection, the Bayesian evidences of the models have to be evaluated and compared. Calculating the evidence can be computationally challenging, in particular when using Monte-Carlo Markov Chains. Therefore, in order to calculate the posterior distributions and the evidence, we use the nested-sampling algorithm [50] as implemented in `pymultinest` [51, 52]. We follow the authors' recommendations and use different sampling efficiencies for evidence evaluation and parameter estimation (`sampling_efficiency` = 0.3 and 0.8 respectively). We used 1000 live points, and a tolerance factor of 1. We checked that the tolerance factor does not affect too much the results.

The priors are shown in Table II. As for h , because of its crucial role in this work, we choose rather wide, uninformative priors. For the other parameters associated to dark energy, we base our priors on physical properties of existing dark energy models, for example the difficulty to obtain realistic phantom models with $w \ll -1$. Finally, we take the priors $\omega_\lambda \in [-4, 0]$, see Figs. 3 and 4 of section III.

An elegant way to compare two models (say model M_1 and the null hypothesis M_0) with different degrees of freedom is to compute the posterior ratio

$$\frac{\Pr(M_1|D)}{\Pr(M_0|D)} = \frac{\Pr(D|M_1) \Pr(M_1)}{\Pr(D|M_0) \Pr(M_0)} \quad (48)$$

$$= \frac{\mathcal{Z}_1}{\mathcal{Z}_0} \equiv K. \quad (49)$$

In (49) we assume $\Pr(M_1) = \Pr(M_0)$. Therefore, $K > 1$ shows a preference for model 1 over model 0. The value of K gives the degree of preference for one model over the other. Several scales have been used, such as the Jeffreys scale, although the latter should be taken as an indication and interpreted with caution.

a. The data The quantities ω_m and ω_r are kept to their fiducial Planck value, and thus so are r_s and r_d . We vary h and the parameters ω_λ , w_X associated with dark energy and obtain $\theta_{\text{s,model}}$ for each set of free parameters which is then compared to $\theta_{\text{s,Planck}}$ and gives us a likelihood for θ_s . In addition, we used the 1048 distance modulus measurements from the Pantheon SNIa compilation [53], and the baryon acoustic oscillations (BAO) from the BOSS and eBOSS surveys [54, 55]. Since the measurements from the SH0ES project are in tension with

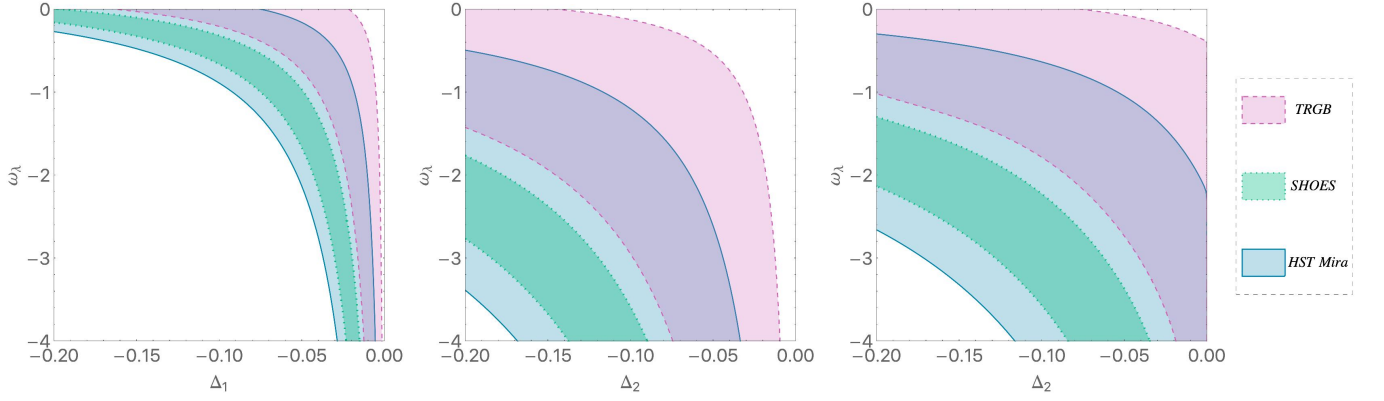


FIG. 4. We show iso- h curves for scenarios I (left), II (middle), and III with $\Delta_1 = -0.04$ (right-hand panel) in the $(\Delta_{1,2}, \omega_\lambda)$ parameter plane. The shaded areas correspond to the following H_0 values (in $\text{km s}^{-1} \text{Mpc}^{-1}$ units): 73.30 ± 4 (HST-Mira) [47], 74.03 ± 1.42 (SH0ES) [48] and 69.8 ± 1.9 (TRGB) [49].

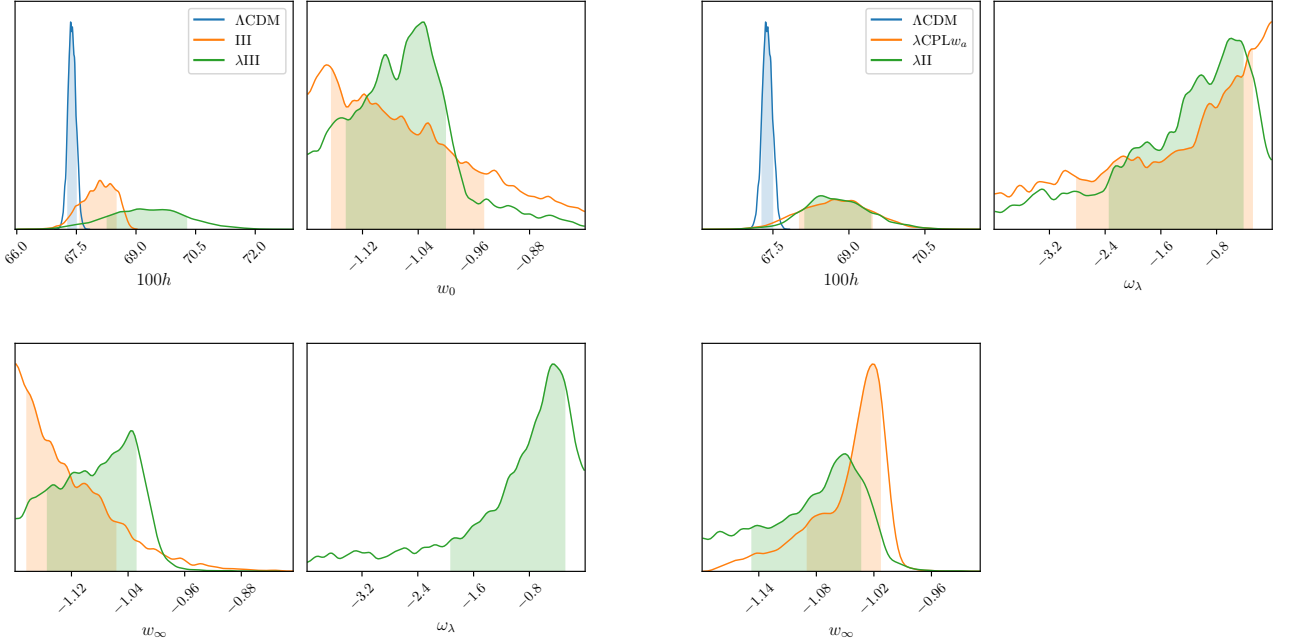


FIG. 5. Marginalized posteriors for different models using SNIa, BAO, θ_s , and H_0 from HST Mira. The central value is the median, and the shaded areas show the 68% credible intervals around it. Left: ΛCDM (blue), III (orange), and λIII (green). Right: ΛCDM (blue), $\lambda\text{CPL}w_a$ (orange), λII (green).

ΛCDM , we instead use a measurement with larger error-bars which is not inconsistent [47]. In general, supernovae show a degeneracy between the absolute magnitude and the Hubble constant. Therefore, SNe Ia alone cannot measure H_0 . However, in this particular study, since we fixed ω_m , choosing a certain value for $\Omega_{m,0}$ uniquely fixes h , therefore we can use SNe Ia data to obtain h . The BAO provide us with $H(z)r_d$ and $d_A(z)/r_d$, where d_A is the angular diameter distance and the sound horizon at the drag epoch r_d is fixed to its Planck value (Table I). The three pairs of data points (d_A/r_d and Hr_d) from BOSS are correlated, and so are the four eBOSS pairs,

and the BAO covariance matrix is thus

$$\mathbf{C}_{\text{BAO}} = \begin{pmatrix} \mathbf{C}_{\text{BOSS}} & 0 \\ 0 & \mathbf{C}_{\text{eBOSS}} \end{pmatrix}. \quad (50)$$

θ_s and H_0 are one data point each, and their associated likelihood is thus trivial. We used flat priors as shown in Table II.

Table III summarizes our results for SN+BAO+ θ_s while in Table IV the H_0 data point from HST-Mira is added. The quoted central values and error-bars correspond to the median and 68% credible intervals around it. We remind the reader that in this analysis, ω_m , ω_b ,

TABLE III. 68% credible intervals for SN+BAO+ θ_s

Model	$100h$	w_0	w_∞ or w_a	ω_λ	$\ln \mathcal{Z}$	K
Λ	$67.382^{+0.107}_{-0.096}$				-532.4	1
w	$68.62^{+0.85}_{-0.83}$	$-1.042^{+0.028}_{-0.029}$		[0]	-533.1	0.54
λw	$68.66^{+0.79}_{-0.75}$	$-1.0102^{+0.0076}_{-0.0203}$		$-0.91^{+0.73}_{-1.88}$	-534.7	0.11
CPL	$68.60^{+0.78}_{-0.84}$	$-1.038^{+0.032}_{-0.029}$	$-0.020^{+0.074}_{-0.055}$	[0]	-532.6	0.83
λ CPL	$68.72^{+0.77}_{-0.87}$	$-1.007^{+0.016}_{-0.028}$	$-0.58^{+0.43}_{-1.11}$	$-0.032^{+0.058}_{-0.044}$	-534.1	0.18
CPL w_0	$68.52^{+0.83}_{-0.85}$	$-1.052^{+0.039}_{-0.038}$	$[-(1 + w_0)]$	[0]	-533.0	0.60
λ CPL w_0	$68.51^{+0.72}_{-0.74}$	$-1.014^{+0.011}_{-0.021}$	$[-(1 + w_0)]$	$-0.84^{+0.65}_{-1.57}$	-534.6	0.12
CPL w_a	$68.34^{+0.39}_{-0.63}$	[-1]	$-0.124^{+0.083}_{-0.050}$	[0]	-532.1	1.48
λ CPL w_a	$68.63^{+0.78}_{-0.75}$	[-1]	$-0.034^{+0.024}_{-0.057}$	$-1.03^{+0.78}_{-1.81}$	-533.1	0.52
I	$68.46^{+0.82}_{-0.83}$	$-1.042^{+0.033}_{-0.032}$	[-1]	[0]	-533.2	0.48
λ I	$68.41^{+0.82}_{-0.75}$	$-1.0092^{+0.0081}_{-0.0242}$	[-1]	$-0.92^{+0.76}_{-1.92}$	-534.8	0.093
II	$67.86^{+0.21}_{-0.34}$	[-1]	$-1.127^{+0.090}_{-0.053}$	[0]	-532.2	1.33
λ II	$68.58^{+0.66}_{-0.59}$	[-1]	$-1.059^{+0.035}_{-0.070}$	$-1.15^{+0.75}_{-1.76}$	-532.1	1.36
III	$67.93^{+0.47}_{-0.50}$	$-1.04^{+0.14}_{-0.11}$	$-1.128^{+0.092}_{-0.049}$	[0]	-532.3	1.20
λ III	$68.93^{+1.03}_{-0.89}$	$-1.046^{+0.070}_{-0.083}$	$-1.090^{+0.054}_{-0.068}$	$-0.65^{+0.43}_{-0.95}$	-531.4	2.96

TABLE IV. 68% credible intervals for SN+BAO+ $\theta_s + H_0$ (HST Mira) - ω_λ priors

Model	$100h$	w_0	w_∞ or w_a	ω_λ	$\ln \mathcal{Z}$	K
Λ	$67.386^{+0.105}_{-0.099}$				-533.5	1
w	$68.83^{+0.82}_{-0.83}$	$-1.049^{+0.028}_{-0.027}$		[0]	-533.7	0.82
λw	$68.81^{+0.86}_{-0.77}$	$-1.0122^{+0.0086}_{-0.0251}$		$-0.81^{+0.66}_{-1.75}$	-535.4	0.16
CPL	$68.77^{+0.75}_{-0.80}$	$-1.044^{+0.031}_{-0.028}$	$-0.020^{+0.072}_{-0.057}$	[0]	-533.3	1.26
λ CPL	$68.75^{+0.84}_{-0.78}$	$-1.005^{+0.015}_{-0.022}$	$-0.035^{+0.053}_{-0.042}$	$-0.71^{+0.52}_{-1.26}$	-534.8	0.30
CPL w_0	$68.71^{+0.82}_{-0.83}$	$-1.061^{+0.038}_{-0.037}$	$[-(1 + w_0)]$	[0]	-533.7	0.87
λ CPL w_0	$68.72^{+0.83}_{-0.93}$	$-1.016^{+0.012}_{-0.033}$	$[-(1 + w_0)]$	$-0.72^{+0.58}_{-1.64}$	-535.3	0.18
CPL w_a	$68.42^{+0.35}_{-0.48}$	[-1]	$-0.134^{+0.063}_{-0.044}$	[0]	-532.8	1.99
λ CPL w_a	$68.76^{+0.70}_{-0.73}$	[-1]	$-0.035^{+0.022}_{-0.054}$	$-1.12^{+0.83}_{-1.69}$	-533.7	0.81
I	$68.67^{+0.80}_{-0.82}$	$-1.050^{+0.032}_{-0.031}$	[-1]	[0]	-533.9	0.69
λ I	$68.51^{+1.09}_{-0.77}$	$-1.0096^{+0.0076}_{-0.0272}$	[-1]	$-0.96^{+0.80}_{-1.92}$	-535.6	0.13
II	$67.89^{+0.18}_{-0.30}$	[-1]	$-1.137^{+0.083}_{-0.044}$	[0]	-533.1	1.53
λ II	$68.73^{+0.70}_{-0.60}$	[-1]	$-1.074^{+0.040}_{-0.073}$	$-1.09^{+0.67}_{-1.24}$	-532.6	2.54
III	$68.09^{+0.41}_{-0.50}$	$-1.077^{+0.131}_{-0.087}$	$-1.137^{+0.080}_{-0.045}$	[0]	-533.1	1.52
λ III	$69.28^{+0.99}_{-1.00}$	$-1.063^{+0.062}_{-0.080}$	$-1.083^{+0.054}_{-0.071}$	$-0.74^{+0.45}_{-1.18}$	-533.3	1.31

N_{eff} , and $\sum m_\nu$ are fixed to their Planck value, and thus so are r_s and r_d (see Table I).

Fig 5 shows the posterior distributions of the parameters for models Λ CDM, III, and λ III (left-hand panel), and Λ CDM, λ CPL w_a , and λ II (right-hand panel). Model III shows preference for a higher value of h , and adding a negative λ pushes h even higher, although this is not sufficient to reconcile it with the SH0ES value. An interesting property of the negative cosmological constant is that it allows to satisfy the observational constraints with an equation of state which is less phantom. This is clearly seen in particular for scenario w , where the addition of λ shifts the central value of w_0 from -1.049 to -1.0122. We

note that given our priors on w_0 and w_∞ , the equation of state is not always constrained, as seen for instance for model III. It is also interesting that the best models λ II are those where the phantom behaviour, and hence the departure from Λ CDM, takes place at $z \gtrsim 1$. This suggests new physics appearing at these redshifts rather than at redshifts $z \lesssim 1$ can yield viable models. Models (λ) III fare reasonably well while having an additional departure from Λ CDM at very low redshifts $z \leq 0.1$ but it is clear when we compare them with models (λ) I that their main advantage comes from their phantomness at $z \gtrsim 1$. This seems further supported by the better evidence for (λ) CPL w_a , where $w_0 = -1$ with a phantom behaviour at

higher redshifts ($w_a < 0$), compared to $(\lambda)\text{CPL}w_0$ with w tending asymptotically to -1 and departure from -1 takes place essentially at low redshifts. Note that $\text{CPL}w_a$ models have the best evidence for $\lambda = 0$ while models II have the highest evidence for $\lambda \neq 0$ (λII). Interestingly $\lambda\text{CPL}w_a$ lowers the evidence compared to $\text{CPL}w_a$. As we have said earlier, perhaps with the exception of the models λII , the higher evidence compared to ΛCDM is not decisive and should be interpreted with caution.

V. SUMMARY AND CONCLUSION

In this work we have considered the possibility that the dark energy sector contains a negative cosmological constant λ . Indeed theoretical considerations from high energy physics suggest the possible presence of a negative cosmological constant rather than a positive one. This constitutes a radical change as in that case, and contrary to a positive cosmological constant Λ , this constant cannot produce the late-time accelerated expansion rate and a more sophisticated dark sector is required. The universe acceleration is produced here by the X-component. Clearly the presence of λ can affect the expansion history and we have studied the viability of these models, also when a high H_0 is considered.

While as we have shown some models can achieve a higher H_0 when the equation of state of the X-component w_X is of the phantom type – this is of course a generic property not restricted to $\lambda \neq 0$ – we have investigated whether these models are viable when SNIa and BAO data are taken into account. We find indeed that most of our models are viable with a fair evidence for the models λII . Taking into account the H_0 value of the HST-mira experiment reinforces the evidence of the models λII , reaching a value $h \approx 0.7$ but not higher. Hence while these models do alleviate the H_0 tension, a value for H_0 substantially higher would rule them out. We note also that the $\text{CPL}w_a$ models are the best models for $\lambda = 0$ while the presence of a non vanishing λ lowers the evidence for $\lambda\text{CPL}w_a$ versus $\text{CPL}w_a$. It is further inter-

esting that the best models λII are equal to ΛCDM on $z \leq 1$ and of the phantom type only at higher redshifts.

The constant λ will manifest itself in a very explicit way in another context, namely the future evolution of our Universe. Considering for concreteness a constant w_X , it is clear that an equation of state $-1 < w_X$, sufficiently negative in order to produce an accelerated expansion rate today, will necessarily produce a transient acceleration stage. It will then eventually lead to a recollapsing universe. We have found the analytical expression for the scale factor $a(t)$ in the regime around the turning point when dust-like matter is negligible compared to the dark sector. On the other hand if the X-component is of the phantom type, $w_X < -1$, our Universe will end in a Big Rip as expected and we have found here too an analytical fit for $a(t)$ valid in the asymptotic region when dust-like matter becomes negligible compared to λ while the latter is not yet negligible compared to the X-component.

Suggested by high energy physics, the possibility to have a negative cosmological constant is worth investigating as it challenges our intuition about the phenomenology of cosmological models. If this negative cosmological constant is substantial enough to affect the cosmic expansion history like in those models investigated here, a high value for H_0 could be a decisive test.

ACKNOWLEDGMENTS

R.G. is supported by FONDECYT project No 1171384. B. L. would like to acknowledge the support of the National Research Foundation of Korea (NRF-2019R1I1A1A01063740). This work benefited from a high performance computing cluster (Seondeok) at the Korea Astronomy and Space Science Institute. This research made use of Astropy, a community-developed core Python package for Astronomy [56, 57], ChainConsumer [58], matplotlib, a Python library for publication quality graphics [59], SciPy [60], NumPy [61]

-
- [1] V. Sahni and A. A. Starobinsky, *Int. J. Mod. Phys. D* **9**, 373 (2000), [arXiv:astro-ph/9904398 \[astro-ph\]](#).
 - [2] P. J. E. Peebles and B. Ratra, *Rev. Mod. Phys.* **75**, 559 (2003), [arXiv:astro-ph/0207347 \[astro-ph\]](#).
 - [3] T. Padmanabhan, *Phys. Rept.* **380**, 235 (2003), [arXiv:hep-th/0212290 \[hep-th\]](#).
 - [4] E. J. Copeland, M. Sami, and S. Tsujikawa, *Int. J. Mod. Phys. D* **15**, 1753 (2006), [arXiv:hep-th/0603057 \[hep-th\]](#).
 - [5] D. H. Weinberg, M. J. Mortonson, D. J. Eisenstein, C. Hirata, A. G. Riess, and E. Rozo, *Phys. Rept.* **530**, 87 (2013), [arXiv:1201.2434 \[astro-ph.CO\]](#).
 - [6] L. Amendola *et al.* (Euclid Theory Working Group), *Living Rev. Rel.* **16**, 6 (2013), [arXiv:1206.1225 \[astro-ph.CO\]](#).
 - [7] J. S. Bullock and M. Boylan-Kolchin, *Ann. Rev. Astron. Astrophys.* **55**, 343 (2017), [arXiv:1707.04256 \[astro-ph.CO\]](#).
 - [8] M. Raveri and W. Hu, *Phys. Rev. D* **99**, 043506 (2019), [arXiv:1806.04649 \[astro-ph.CO\]](#).
 - [9] L. Verde, J. L. Bernal, A. F. Heavens, and R. Jimenez, *Mon. Not. Roy. Astron. Soc.* **467**, 731 (2017), [arXiv:1607.05297 \[astro-ph.CO\]](#).
 - [10] J. L. Bernal, L. Verde, and A. G. Riess, *JCAP* **10**, 019 (2016), [arXiv:1607.05617 \[astro-ph.CO\]](#).
 - [11] B. L'Huillier and A. Shafieloo, *J. Cosmology Astropart. Phys.* **2017**, 015 (2017), [arXiv:1606.06832 \[astro-ph.CO\]](#).
 - [12] A. Shafieloo, B. L'Huillier, and A. A. Starobinsky, *Phys. Rev. D* **98**, 083526 (2018), [arXiv:1804.04320 \[astro-ph.CO\]](#).

- [13] L. Verde, T. Treu, and A. Riess (2019) [arXiv:1907.10625 \[astro-ph.CO\]](#).
- [14] Planck Collaboration, P. A. R. Ade, N. Aghanim, M. Arnaud, M. Ashdown, J. Aumont, C. Baccigalupi, A. J. Banday, R. B. Barreiro, J. G. Bartlett, *et al.*, **A&A** **594**, A13 (2016), [arXiv:1502.01589 \[astro-ph.CO\]](#).
- [15] R. Cardenas, T. Gonzalez, Y. Leiva, O. Martin, and I. Quiros, **Phys. Rev. D** **67**, 083501 (2003), [arXiv:astro-ph/0206315 \[astro-ph\]](#).
- [16] L. Visinelli, S. Vagnozzi, and U. Danielsson, **Symmetry** **11**, 1035 (2019), [arXiv:1907.07953 \[astro-ph.CO\]](#).
- [17] G. Ye and Y.-S. Piao, **Phys. Rev. D** **101**, 083507 (2020), [arXiv:2001.02451 \[astro-ph.CO\]](#).
- [18] Ö. Akarsu, J. D. Barrow, L. A. Escamilla, and J. A. Vazquez, **Phys. Rev. D** **101**, 063528 (2020), [arXiv:1912.08751 \[astro-ph.CO\]](#).
- [19] B. Boisseau, H. Giacomini, D. Polarski, and A. Starobinsky, **JCAP** **07**, 002 (2015), [arXiv:1504.07927 \[gr-qc\]](#).
- [20] J. A. Vazquez, S. Hee, M. P. Hobson, A. N. Lasenby, M. Ibison, and M. Bridges, **JCAP** **1807**, 062 (2018), [arXiv:1208.2542 \[astro-ph.CO\]](#).
- [21] J. Grande, J. Sola, and H. Stefancic, **JCAP** **0608**, 011 (2006), [arXiv:gr-qc/0604057 \[gr-qc\]](#).
- [22] K. Dutta, Ruchika, A. Roy, A. A. Sen, and M. M. Sheikh-Jabbari, **Gen. Rel. Grav.** **52**, 15 (2020), [arXiv:1808.06623 \[astro-ph.CO\]](#).
- [23] G. Alestas, L. Kazantzidis, and L. Perivolaropoulos, **Phys. Rev. D** **101**, 123516 (2020), [arXiv:2004.08363 \[astro-ph.CO\]](#).
- [24] E. Ó Colgáin, M. H. van Putten, and H. Yavartanoo, **Phys. Lett. B** **793**, 126 (2019), [arXiv:1807.07451 \[hep-th\]](#).
- [25] V. Poulin, T. L. Smith, T. Karwal, and M. Kamionkowski, **Phys. Rev. Lett.** **122**, 221301 (2019), [arXiv:1811.04083 \[astro-ph.CO\]](#).
- [26] K. Vattis, S. M. Koushiappas, and A. Loeb, **Phys. Rev. D** **99**, 121302 (2019), [arXiv:1903.06220 \[astro-ph.CO\]](#).
- [27] P. Agrawal, G. Obied, and C. Vafa, *arXiv e-prints*, [arXiv:1906.08261 \(2019\)](#), [arXiv:1906.08261 \[astro-ph.CO\]](#).
- [28] X. Li and A. Shafieloo, **ApJ** **883**, L3 (2019), [arXiv:1906.08275 \[astro-ph.CO\]](#).
- [29] S. Vagnozzi, **Phys. Rev. D** **102**, 023518 (2020), [arXiv:1907.07569 \[astro-ph.CO\]](#).
- [30] E. Di Valentino, A. Melchiorri, O. Mena, and S. Vagnozzi, **Physics of the Dark Universe** **30**, 100666 (2020), [arXiv:1908.04281 \[astro-ph.CO\]](#).
- [31] M. Demianski, E. Piedipalumbo, D. Sawant, and L. Amati, *arXiv e-prints*, [arXiv:1911.08228 \(2019\)](#), [arXiv:1911.08228 \[astro-ph.CO\]](#).
- [32] L. A. Anchordoqui, I. Antoniadis, D. Lüst, J. F. Soriano, and T. R. Taylor, **Phys. Rev. D** **101**, 083532 (2020), [arXiv:1912.00242 \[hep-th\]](#).
- [33] G. Benevento, W. Hu, and M. Raveri, **Phys. Rev. D** **101**, 103517 (2020), [arXiv:2002.11707 \[astro-ph.CO\]](#).
- [34] A. Hernández-Almada, G. Leon, J. Magaña, M. A. García-Aspeitia, and V. Motta, **MNRAS** **497**, 1590 (2020), [arXiv:2002.12881 \[astro-ph.CO\]](#).
- [35] W. E. V. Barker, A. N. Lasenby, M. P. Hobson, and W. J. Handley, **Phys. Rev. D** **102**, 024048 (2020), [arXiv:2003.02690 \[gr-qc\]](#).
- [36] K. Jedamzik and L. Pogosian, *arXiv e-prints*, [arXiv:2004.09487 \(2020\)](#), [arXiv:2004.09487 \[astro-ph.CO\]](#).
- [37] M. Ballardini, M. Braglia, F. Finelli, D. Paoletti, A. A. Starobinsky, and C. Umiltà, *arXiv e-prints*, [arXiv:2004.14349 \(2020\)](#), [arXiv:2004.14349 \[astro-ph.CO\]](#).
- [38] A. Banerjee, H. Cai, L. Heisenberg, E. Ó. Colgáin, M. M. Sheikh-Jabbari, and T. Yang, *arXiv e-prints*, [arXiv:2006.00244 \(2020\)](#), [arXiv:2006.00244 \[astro-ph.CO\]](#).
- [39] J. Sola, A. Gomez-Valent, J. d. C. Perez, and C. Moreno-Pulido, *arXiv e-prints* (2020), [arXiv:2006.04273 \[astro-ph.CO\]](#).
- [40] T. Sekiguchi and T. Takahashi, *arXiv e-prints*, [arXiv:2007.03381 \(2020\)](#), [arXiv:2007.03381 \[astro-ph.CO\]](#).
- [41] H. Benaoum, W. Yang, S. Pan, and E. Di Valentino, *arXiv e-prints* (2020), [arXiv:2008.09098 \[gr-qc\]](#).
- [42] Planck Collaboration, N. Aghanim, Y. Akrami, M. Ashdown, J. Aumont, C. Baccigalupi, M. Ballardini, A. J. Banday, R. B. Barreiro, N. Bartolo, *et al.*, *arXiv e-prints*, [arXiv:1807.06209 \(2018\)](#), [arXiv:1807.06209 \[astro-ph.CO\]](#).
- [43] L. Knox and M. Millea, **Phys. Rev. D** **101**, 043533 (2020), [arXiv:1908.03663 \[astro-ph.CO\]](#).
- [44] E. Komatsu, K. M. Smith, J. Dunkley, C. L. Bennett, B. Gold, G. Hinshaw, N. Jarosik, D. Larson, M. R. Nolta, L. Page, *et al.*, **ApJS** **192**, 18 (2011), [arXiv:1001.4538 \[astro-ph.CO\]](#).
- [45] M. Chevallier and D. Polarski, **Int. J. Mod. Phys. D** **10**, 213 (2001), [arXiv:gr-qc/0009008](#).
- [46] E. V. Linder, **Phys. Rev. Lett.** **90**, 091301 (2003), [arXiv:astro-ph/0208512](#).
- [47] C. D. Huang, A. G. Riess, W. Yuan, L. M. Macri, N. L. Zakamska, S. Casertano, P. A. Whitelock, S. L. Hoffmann, A. V. Filippenko, and D. Scolnic, **ApJ** **889**, 5 (2020), [arXiv:1908.10883 \[astro-ph.CO\]](#).
- [48] A. G. Riess, S. Casertano, W. Yuan, L. M. Macri, and D. Scolnic, **Astrophys. J.** **876**, 85 (2019), [arXiv:1903.07603 \[astro-ph.CO\]](#).
- [49] W. L. Freedman, B. F. Madore, D. Hatt, T. J. Hoyt, I. S. Jang, R. L. Beaton, C. R. Burns, M. G. Lee, A. J. Monson, J. R. Neeley, M. M. Phillips, J. A. Rich, and M. Seibert, **ApJ** **882**, 34 (2019), [arXiv:1907.05922 \[astro-ph.CO\]](#).
- [50] J. Skilling, in *American Institute of Physics Conference Series*, American Institute of Physics Conference Series, Vol. 735, edited by R. Fischer, R. Preuss, and U. V. Toussaint (2004) pp. 395–405.
- [51] F. Feroz, M. P. Hobson, and M. Bridges, **MNRAS** **398**, 1601 (2009), [arXiv:0809.3437 \[astro-ph\]](#).
- [52] J. Buchner, A. Georgakakis, K. Nandra, L. Hsu, C. Rangel, M. Brightman, A. Merloni, M. Salvato, J. Donley, and D. Kocevski, **A&A** **564**, A125 (2014), [arXiv:1402.0004 \[astro-ph.HE\]](#).
- [53] D. M. Scolnic, D. O. Jones, A. Rest, Y. C. Pan, R. Chornock, R. J. Foley, M. E. Huber, R. Kessler, G. Narayan, A. G. Riess, *et al.*, **ApJ** **859**, 101 (2018), [arXiv:1710.00845 \[astro-ph.CO\]](#).
- [54] S. Alam, M. Ata, S. Bailey, F. Beutler, D. Bizyaev, J. A. Blazek, A. S. Bolton, J. R. Brownstein, A. Burden, C.-H. Chuang, *et al.*, **MNRAS** **470**, 2617 (2017), [arXiv:1607.03155 \[astro-ph.CO\]](#).
- [55] G.-B. Zhao, Y. Wang, S. Saito, D. Wang, A. J. Ross, F. Beutler, J. N. Grieb, C.-H. Chuang, F.-S. Kitaura, S. Rodriguez-Torres, *et al.*, **MNRAS** **466**, 762 (2017),

- [arXiv:1607.03153 \[astro-ph.CO\]](#).
- [56] Astropy Collaboration, A. M. Price-Whelan, B. M. Sipőcz, H. M. Günther, P. L. Lim, S. M. Crawford, S. Conseil, D. L. Shupe, M. W. Craig, N. Dencheva, *et al.*, *AJ* **156**, 123 (2018), [arXiv:1801.02634 \[astro-ph.IM\]](#).
 - [57] Astropy Collaboration, T. P. Robitaille, E. J. Tollerud, P. Greenfield, M. Droettboom, E. Bray, T. Aldcroft, M. Davis, A. Ginsburg, A. M. Price-Whelan, *et al.*, *A&A* **558**, A33 (2013), [arXiv:1307.6212 \[astro-ph.IM\]](#).
 - [58] S. R. Hinton, *The Journal of Open Source Software* **1**, 00045 (2016).
 - [59] J. D. Hunter, *Computing In Science & Engineering* **9**, 90 (2007).
 - [60] P. Virtanen, R. Gommers, T. E. Oliphant, M. Haberland, T. Reddy, D. Cournapeau, E. Burovski, P. Peterson, W. Weckesser, J. Bright, *et al.*, *Nature Methods* **17**, 261 (2020).
 - [61] S. Van Der Walt, S. C. Colbert, and G. Varoquaux, *Computing in Science & Engineering* **13**, 22 (2011).